A comparative study of small field total scatter factors and dose profiles using plastic scintillation detectors and other stereotactic dosimeters: The case of the CyberKnife

Jonathan Morin
Département de Physique, de Génie Physique et d'Optique, Université Laval, Québec, Québec G1K 7P4, Canada and Département de Radio-Oncologie, Hôtel-Dieu de Québec, Centre Hospitalier Universitaire de Québec, Québec G1R 2J6, Canada

Dominic Béliveau-Nadeau
Département de Radio-Oncologie, Hôpital Notre-Dame, Centre Hospitalier de l'Université de Montréal, Montréal H2L 2T4, Canada

Eunah Chung and Jan Seuntjens
Medical Physics Unit, McGill University, Montreal General Hospital (L5-113), 1650 Cedar Avenue, Montreal, Quebec H3G 1A4, Canada

Dany Thériault
Département de Radio-Oncologie, Hôtel-Dieu de Québec, Centre Hospitalier Universitaire de Québec, Québec G1R 2J6, Canada

Louis Archambault
Département de Physique, de Génie Physique et d'Optique, Université Laval, Québec, Québec G1K 7P4, Canada and Département de Radio-Oncologie, Hôtel-Dieu de Québec, Centre Hospitalier Universitaire de Québec, Québec G1R 2J6, Canada

Sam Beddar
Department of Radiation Physics, Unit 94, The University of Texas MD Anderson Cancer Center, 1515 Holcombe Boulevard, Houston, Texas 77030

Luc Beaulieu[a)]
Département de Physique, de Génie Physique et d'Optique, Université Laval, Québec, Québec G1K 7P4, Canada and Département de Radio-Oncologie, Hôtel-Dieu de Québec, Centre Hospitalier Universitaire de Québec, Québec G1R 2J6, Canada

(Received 13 July 2012; revised 24 November 2012; accepted for publication 30 November 2012; published 4 January 2013)

Purpose: Small-field dosimetry is challenging, and the main limitations of most dosimeters are insufficient spatial resolution, water nonequivalence, and energy dependence. The purpose of this study was to compare plastic scintillation detectors (PSDs) to several commercial stereotactic dosimeters by measuring total scatter factors and dose profiles on a CyberKnife system.
Methods: Two PSDs were developed, having sensitive volumes of 0.196 and 0.785 mm^3, and compared with other detectors. The spectral discrimination method was applied to subtract Čerenkov light from the signal. Both PSDs were compared to four commercial stereotactic dosimeters by measuring total scatter factors, namely, an IBA dosimetry stereotactic field diode (SFD), a PTW 60008 silicon diode, a PTW 60012 silicon diode, and a microLion. The measured total scatter factors were further compared with those of two independent Monte Carlo studies. For the dose profiles, two commercial detectors were used for the comparison, i.e., a PTW 60012 silicon diode and Gafchromics EBT2. Total scatter factors for a CyberKnife system were measured in circular fields with diameters from 5 to 60 mm. Dose profiles were measured for the 5- and 60-mm cones. The measurements were performed in a water tank at a 1.5-cm depth and an 80-cm source-axis distance.
Results: The total scatter factors measured using all the detectors agreed within 1% with the Monte Carlo values for cones of 20 mm or greater in diameter. For cones of 10–20 mm in diameter, the PTW 60008 silicon diode was the only dosimeter whose measurements did not agree within 1% with the Monte Carlo values. For smaller fields (<10 mm), each dosimeter type showed different behaviors. The silicon diodes over-responded because of their water nonequivalence; the microLion and 1.0-mm PSD under-responded because of a volume-averaging effect; and the 0.5-mm PSD was the only detector within the uncertainties of the Monte Carlo simulations for all the cones. The PSDs, the PTW 60012 silicon diode, and the Gafchromics EBT2 agreed within 2% and 0.2 mm (gamma evaluation) for the measured dose profiles except in the tail of the 60-mm cone.
Conclusions: Silicon diodes can be used to accurately measure small-field dose profiles but not to measure total scatter factors, whereas PSDs can be used to accurately measure both. The

authors' measurements show that the use of a 1.0-mm PSD resulted in a negligible volume-averaging effect (under-response of ≈1%) down to a field size of 5 mm. Therefore, PSDs are strong candidates to become reference radiosurgery detectors for beam characterization and quality assurance measurements. © *2013 American Association of Physicists in Medicine*. [http://dx.doi.org/10.1118/1.4772190]

Key words: plastic scintillation detectors, CyberKnife system, total scatter factors, dose profiles, stereotactic radiosurgery

I. INTRODUCTION

Stereotactic radiosurgery was introduced by Lars Leksell in the 1950s when he suggested the use of a high radiation dose and stereotactic frame to treat small regions in the human brain. Since then, several treatment devices have been developed, such as the Gamma Knife (Elekta, Stockholm, Sweden), Novalis radiosurgery system (Varian Medical Systems, Palo Alto, CA, USA, and Brainlab, Munich, Germany), the CyberKnife system (Accuray, Sunnyvale, CA, USA), and stereotactic accessories for conventional linear accelerator. The CyberKnife system offers several advantages over the other devices: it is a frameless, real-time image-guided, and nonisocentric treatment modality. It consists of a 6-MV linear accelerator mounted on a robotic manipulator arm that has six degrees of freedom. The CyberKnife system can deliver small fields using 12 circular tungsten cones that are 5–60 mm in diameter (i.e., 5, 7.5, 10, 12.5, 15, 20, 25, 30, 35, 40, 50, and 60 mm). Podgorsak[1] recommended thresholds of ±1 mm and ±5% for the positioning and delivered dose accuracy, respectively, using radiosurgery techniques. Some studies have demonstrated that the CyberKnife system meets these thresholds[2,3] even in the absence of a stereotactic frame.

Each radiosurgery treatment apparatus should be modeled into the treatment planning system[4] because some parameters are specific to each accelerator. Francescon *et al.*[5] determined that the parameters that have the highest impact on small-field total scatter factors are the electron spot size and the nominal electron energy incident on the target. A change of ±4% was observed on the total scatter factor of the 5-mm cone with a change of ±0.5 mm on the electron spot size.[5] Moreover, conventional dosimeters often underestimate the dose delivered by small radiation fields because of volume-averaging and perturbation effects.[6,7] Spatial resolution is thus an essential property when dealing with small fields because no flat dose region exists, resulting in the delivery of a nonuniform dose throughout the detector.

The greatest challenge associated with small-field dosimetry is the lateral electronic disequilibrium. Its impact on dosimetry has been broadly described in the literature.[4,8–10] In a recently published quality assurance report on robotic radiosurgery, the American Association of Physicists in Medicine Task Group 135 noted that the gold standard detector for TPR, dose profile, and total scatter factor measurements for small-field dosimetry is a diode.[11] However, a sensitive volume medium denser than water, such as silicon, artificially increases the lateral electronic equilibrium at the detector location, whereas a medium that is less dense than water, such as air, reduces it, resulting in over-responses and under-responses, respectively.[8–10] In addition, silicon diodes are energy dependent and, as narrow beam collimation hardens the photon fluence spectrum, the diodes response to water is compromised in small fields.[12] Several types of single-point detector can be used and a comprehensive review on the subject can be found in Jordan (2006).[13]

In this study, we investigated whether plastic scintillation detectors (PSDs) have superior characteristics compared to commercial radiosurgery dosimeters for small-field dosimetry due to their water equivalence and the good spatial resolution possible to achieve. PSDs have been widely studied and showed excellent results for dosimetry in small and nonstandard radiation fields used in radiotherapy.[14–19] In this work, we compared two PSDs of different dimensions with several commercial stereotactic dosimeters by measuring total scatter factors and dose profiles of a CyberKnife system. The measured total scatter factors were further compared with Monte Carlo dose calculations in water. Finally, correction factors were experimentally extracted for the commercial stereotactic detectors using the 0.5-mm PSD as the reference detector.

II. MATERIALS AND METHODS

II.A. Detectors

No commercial detector possesses all the properties necessary to perform accurate dosimetry in small fields; thus, none can be used as a reference without correction factors. We compared the total scatter factors of six detectors and compared the dose profiles of four detectors to characterize the strengths and weaknesses of each dosimeter for small-field dosimetry. All the detectors used are described below.

II.A.1. Stereotactic field diode

The stereotactic field diode (SFD; IBA Dosimetry, Schwarzenbruck, Germany) was developed specifically for small-field dosimetry by leaving the sensitive volume unshielded. The absence of a shield behind the silicon chip results in an important over-response to low-energy scattered photons, up to 15% in large fields. The sensitive volume is cylindrical with a diameter of 0.6 mm and a length of 0.06 mm (0.017 mm^3). Precautions must be taken with this dosimeter because the signal increases with delivered dose to the sensitive volume. This signal instability was also observed by Derreumaux *et al.*[20]

II.A.2. PTW 60008 silicon diode

The PTW 60008 silicon diode (Physikalisch-Technische Werkstätten [PTW], Freiburg, Germany) is shielded against low-energy scattered photons by a thin metallic plate. Shielded diodes are not recommended to perform small-field dose measurements because they result in unwanted filtration of the low energy spectrum and an over response from electron scattering.[21] However, this detector was included in this study because, historically, it has been widely used for small-field quality assurance (QA) measurements. The sensitive volume is cylindrical with a diameter of 1.13 mm and length of 0.025 mm (0.025 mm^3).

II.A.3. PTW 60012 silicon diode

The PTW 60012 silicon diode (Physikalisch-Technische Werkstätten) was developed to succeed the PTW 60008 silicon diode for small-field dosimetry. The dimensions of the PTW 60012 are identical to those of the PTW 60008; however, the PTW 60012 silicon diode is unshielded, so it performs well for small-field measurements but not for large-field measurements. This dosimeter was used in the commissioning of the CyberKnife radiosurgery system used in the present study.

II.A.4. MicroLion chamber

The microLion (Physikalisch-Technische Werkstätten) was recently developed specifically for small-field dosimetry. The sensitive volume in this chamber is composed of isooctane (C_8H_{18}) rather than air, enabling the sensitive volume to be reduced to 1.7 mm^3, and a high electrical signal response is conserved for a given dose. The design is a parallel plate chamber with a diameter of 2.5 mm and electrode spacing of 0.35 mm. The entrance window is composed of polystyrene, graphite, and varnish. The central electrode is made of graphite only.

II.A.5. Gafchromic EBT2

Developed in 2009, Gafchromic EBT2 (Ashland, Calvert City, KY, USA) is the second-generation radiochromic film. The active layer is made primarily of hydrogen, carbon, and oxygen and is sandwiched between protective and polyester layers also composed of organic elements. Its overall effective atomic number is 6.84, and its density is 1.2 g/cm^2, making this detector almost water equivalent in the megavoltage energy range, in addition to its energy independence.[22] Gafchromic film is an effective relative dose measurement technique and is often used for dose profile measurements. It has been used to that purpose in the present work. Gafchromic film dosimetry is not a real-time technique, and a long time-consuming procedure is required to extract the results thereof. After irradiations, the films were kept in an opaque envelope for 48 h before being scanned using an Epson Expression 10000XL scanner (Seiko Epson Corporation, Nagano, Japan) in reflection mode. Each film was scanned five times before irradiation to determine the mean background value and five times after irradiation to obtain a mean image. A calibration curve was obtained by irradiating films of the same batch from 0 to 10 Gy with 13 different dose points. Gafgui is a free software program developed by Bouchard and Lacroix to analyze Gafchromic films[23] and was used in the present study. The procedure proposed by Bouchard *et al.*[24] was used to perform the measurements, scan the films, and analyze the images.

II.A.6. PSDs

Two PSDs were developed in this study to compare the volume-averaging effect between two detector sizes. All the characteristics of the two PSDs were identical except their diameters, thus providing different spatial resolutions perpendicular to the radiation beam. The smaller PSD was composed of a cylindrical scintillating fiber (multicladding SCSF-78M, Kuraray Co., Ltd., Tokyo, Japan) with a diameter of 0.5 mm and a length of 1.0 mm coupled with a PMMA optical fiber (Super Eska SH-2001, Mitsubishi, Rayon Co., Ltd., Tokyo, Japan) with a diameter of 0.5 mm and a length of 5 m to guide the scintillation produced to a polychromatic charge-coupled device (CCD) (U2000c, Apogee Imaging System, Roseville, CA, USA). A light collection system was developed to maximize the signal-to-noise ratio (SNR) using an optical lens (Minolta MC Rokkor-X PG, f/# = 1.4, focal length = 50 mm). The larger PSD was composed of a cylindrical scintillating fiber (BCF-12, Saint-Gobain Crystals, Paris, France) with a diameter of 1.0 mm and a length of 1.0 mm coupled with an Eska Premier GH-4001 optical fiber (Mitsubishi, Rayon Co., Ltd., Tokyo, Japan). The sensitive volumes of the smaller and larger PSDs were 0.196 and 0.785 mm^3, respectively. A polyethylene jacket coated the scintillating and optical fibers to insulate them from ambient light. The effective point of measurement of a PSD is considered at the geometric center of the sensitive volume.[25] Figure 1 shows the whole detector and readout assembly.

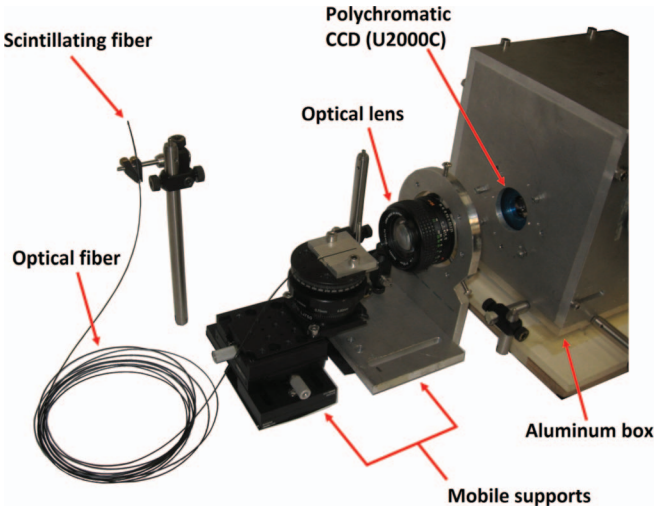

FIG. 1. PSDs were composed of a cylindrical scintillating fiber coupled with a 5 m long collecting optical fiber which had the same diameter. An optical lens was used to focus the light on a CCD chip, which converted input light in electrical current. The CCD was connected to a computer via a USB cable.

II.B. Measurements

Total scatter factors and dose profiles were measured with a 3rd generation CyberKnife radiosurgery system (6 MV, 800 MU/min dose rate) using tungsten cones. A blue phantom water tank (IBA Dosimetry, Schwarzenbruck, Germany) with a spatial position accuracy of ±0.1 mm was used for scanning with all detectors except when using the radiochromic films. The latter were sandwiched between plastic water equivalent slabs (Gammex 457, Gammex, Middleton, USA) at a depth of 1.5 cm with 15 cm of backscattering material. The source-axis distance was 80 cm, and the effective point of measurement of each detector was placed at a depth of 1.5 cm. The effective point of measurement was placed at the center field position in two steps with the 5-mm cone for all the detectors in the water tank. First, the detector was crudely positioned using the laser pointer from the CyberKnife system head. Then, the detector position was fine-tuned by taking measurements at 0.2-mm increments until the maximum signal was found in the x and y directions. The positioning in the z direction was adjusted using offsets with the robotic arm of the water tank to place the effective point of measurement of each detector (provided by the manufacturers) at a depth of 1.5 cm. The uncertainties of the measurements were quoted as one standard deviation (Type A uncertainty) on the repeated measurements for all detectors.

II.B.1. Total scatter factors

Total scatter factors were measured for 10 of the 12 cone sizes available using the CyberKnife system (5, 7.5, 10, 12.5, 15, 20, 30, 40, 50, and 60 mm). Using the formalism proposed by Alfonso *et al.*,[6] the total scatter factor (also called field output factor) $\Omega_{Q_{\text{clin}},Q_{\text{msr}}}^{f_{\text{clin}},f_{\text{msr}}}$ was defined as

$$\Omega_{Q_{\text{clin}},Q_{\text{msr}}}^{f_{\text{clin}},f_{\text{msr}}} = \frac{M_{Q_{\text{clin}}}^{f_{\text{clin}}}}{M_{Q_{\text{msr}}}^{f_{\text{msr}}}} \cdot k_{Q_{\text{clin}},Q_{\text{msr}}}^{f_{\text{clin}},f_{\text{msr}}} = s_{c,p} \cdot k_{Q_{\text{clin}},Q_{\text{msr}}}^{f_{\text{clin}},f_{\text{msr}}}, \quad (1)$$

where f and Q are the collimator size in millimeters and the beam quality. The suffixes clin and msr represent the field of interest (clinical field) and the machine-specific reference (60 mm for a CyberKnife system[6]), respectively. M represents the reading of the detector for the given field, and $k_{Q_{\text{clin}},Q_{\text{msr}}}^{f_{\text{clin}},f_{\text{msr}}}$ represents the correction factor needed to determine the dose to water between f_{clin} and f_{msr} because of the presence of the detector in water (correction factors are discussed in Sec. III.B). The ratio of the readings ($M_{Q_x}^{f_x}$) for f_{clin} to f_{msr} is noted $s_{c,p}$ and is called "measured total scatter factor" for the rest of the paper to simplify the notation. The cone was changed manually between each set of measurements for a given cone, so the CyberKnife system head did not move during the entire measurement sequence.

The silicon diodes, PSDs, and microLion were used with their stems parallel to the beam axis. Silicon diodes necessitate no external bias and their signals were measured using the Fluke Biomedical Model 35040 Advanced Therapy Dosimeter electrometer (Fluke Biomedical, Everett, WA, USA). The signals of the microLion were measured using the Keithley 6517A electrometer (Keithley, Cleveland, OH, USA), which can provide ±1000 V, because an external bias of –800 V is needed with this chamber type to minimize the ion recombination.[26] PSDs produce visible light rather than an electrical current; thus, a polychromatic Apogee U2000c charge-coupled device with a light collection system were used, as explained in Sec. II.A.6. All measurements were performed three times using each detector except the PSDs, for which five measurements were performed. The dose delivered for all measurements was 200 monitor units (MU), which was equivalent to 200 cGy (1 cGy/MU to ≈0.08 MU/pulse where the latter was estimated from the manufacturer's values) using the 60-mm cone under these conditions.

As mentioned in Sec. II.A.1, a special precaution was necessary with the SFD to account for the signal increase with the total dose delivered to the sensitive volume (estimated to 1%/Gy when normalized to the dose delivered using the 60-mm cone). The approach taken consisted of performing a measurement with the reference cone (60 mm) before and after the measurements with the cones of interest (5–50 mm). The signal measured with each cone of interest was normalized to the average of these two measurements to account for the drift of the SFD response.

The 0.5 mm-PSD was used as a reference dosimeter to determine correction factors for the measured total scatter factors of the three smallest cones using the other dosimeters studied in this work.

II.B.2. Dose profiles

To compare the two extreme conditions encountered with a CyberKnife system, we measured dose profiles using the 5- and 60-mm cones. The center of the radiation field was used as the normalization point of dose. The dose profiles were measured using the two PSDs, the PTW 60012 silicon diode, and the radiochromic films. The PSDs and the diode were used with their stems parallel to the radiation field axis to provide the best spatial resolution for the smaller PSD, whereas the films were placed perpendicularly. Moreover, the orientation of the diode with respect to the radiation beam may have an impact when performing dose profile measurements.[27] In this study, all measurements were performed with the diode parallel to the beam direction (i.e., vertical in the water phantom), which should guarantee symmetrical dose profile measurements. The silicon diode dose profile measurements were performed during the commissioning of the CyberKnife system by using the dynamic scan mode of the water tank and were averaged over several directions. The PSDs dose profile measurements were performed point by point because no synchronization system has been developed between the water tank's positioning controller and the CCD to use the dynamic scan mode. The dose of each point was measured three times delivering 100 MU/measurement and 50 MU/measurement for the 5- and 60-mm cones, respectively. The increment between each point was 0.3 mm throughout the 5-mm cone dose profile. With the 60-mm cone, the increments were 1 mm from the center to 15 and 0.3 mm from 15 to 37.5 mm. The Gafchromic film dose profile measurements consisted of a single irradiation of 200 MU, and several profiles were

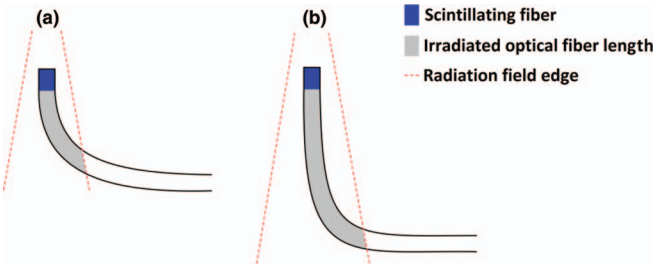

FIG. 2. Čerenkov calibration procedure. Measurements were taken in conditions minimizing (a) and maximizing (b) Čerenkov light to determine b_c/g_c. See Sec. II.C for details.

averaged in different directions. Gamma evaluations were performed for both profiles to quantify the agreement between the detectors, and the detector of reference was the 0.5-mm PSD corrected for the volume-averaging effect.

II.C. Čerenkov calibration procedure

The PMMA optical fiber produces its own visible light spectrum when irradiated, contaminating dose readings.[28,29] Some techniques have been developed to subtract this unwanted signal, including the subtraction of Čerenkov light using a background optical fiber not coupled with a scintillating fiber,[30] spectral discrimination using two different wavelength channels to measure light signal,[31–33] and a temporal method to measure scintillation between the pulses of the accelerator.[34,35] The spectral discrimination procedure proposed by Guillot *et al.*[33] was used in the present study (method C). This method requires the knowledge of the Čerenkov spectrum expressed as b_c/g_c, where b_c and g_c are pure Čerenkov light collected in the two wavelength channels used (i.e., the blue and green channels of the U2000c polychromatic CCD camera in the present study). Only relative dose measurements were performed in the present paper, making it unnecessary to determine the gain factor in cGy/(scintillation unit). We modified the measurement procedure proposed by Guillot *et al.* to determine the Čerenkov spectrum with the detector placed in the same orientation as the measurements of total scatter factors and dose profiles. The calibration procedure represented in Fig. 2 was applied to determine b_c/g_c using the 60-mm cone. Measurements A and B produced the same scintillation signal but not the same Čerenkov signal. By subtracting the signal of measurement A from the signal of measurement B, we obtained pure Čerenkov signal, with which we determined b_c/g_c.

II.D. Reference datasets

The performance of each detector was evaluated by comparing the measured total scatter factors against published data from two independent Monte Carlo studies. In the first Monte Carlo study, Araki[8] simulated total scatter factors ($\Omega^{f_{clin},f_{msr}}_{Q_{clin},Q_{msr}}$) for all 12 available cone diameters on a CyberKnife system. Calculations were further compared with SFD measurements performed at 14 CyberKnife systems located in Japan. Two parameters must be determined to adequately simulate total scatter factors by using Monte Carlo calculations. These parameters are: (1) the electron spot size and (2) the nominal electron energy. The electron spot size is defined as the full width at half maximum of a radial Gaussian distribution and the nominal electron energy is the energy of the electrons incident on the target in the accelerator head. These two parameters were adjusted by Araki by fitting measured and simulated off-axis dose profiles and central axis depth-doses. In the second Monte Carlo study, which is separated in two different papers, Francescon *et al.*[5,36] developed a method to determine these two parameters for any CyberKnife system from measured tissue-phantom ratios and total scatter factors with some specific dosimeters. This method was applied in the present work to determine these parameters for our specific CyberKnife system. Then, calculated total scatter factors were determined with our specific parameters from tables obtained by Francescon *et al.*[5] This latter study focused on the three smallest cones (5, 7.5, and 10 mm), for which the electron spot size and the nominal electron energy incident on the target have the highest impact.

III. RESULTS

III.A. Total scatter factors

The measured total scatter factors normalized to Araki and Francescon using Eq. (2) are presented in Figs. 3 and 4, respectively, and the raw data are presented in Table I. The PTW 60008 silicon diode rendered the worst results with noticeable over-response for cones smaller than 20 mm in diameter. All the silicon diodes over-responded compared with Araki's calculated values in small fields. The 1.0-mm PSD and the microLion measured values agreed with Monte Carlo results

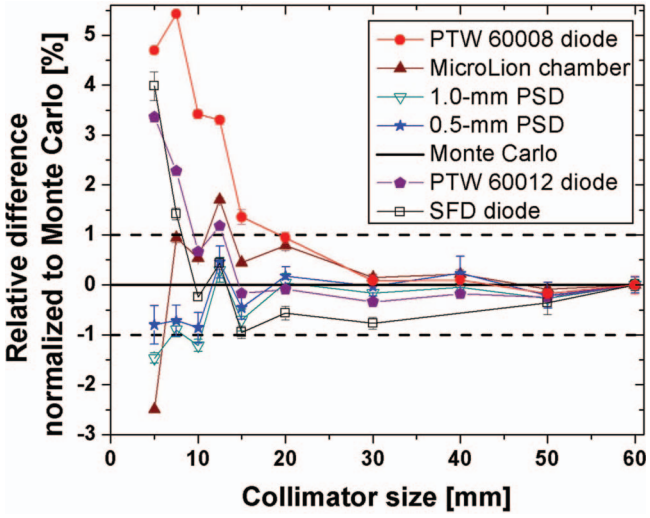

FIG. 3. Relative total scatter factors difference normalized to Monte Carlo [Araki (Ref. 8)]. The y-axis represents the relative total scatter factor difference normalized to Monte Carlo and the x-axis represents the collimator diameter in millimeters. The continuous black line represents the Monte Carlo results and the dotted lines represent 1 standard deviation of the same simulations.

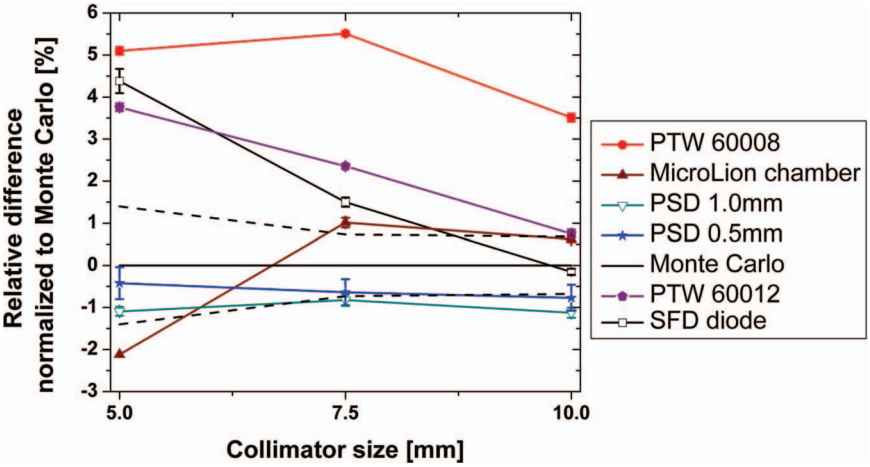

FIG. 4. Relative total scatter factors difference normalized to Monte Carlo [Francescon *et al.* (Ref. 5)]. The y-axis represents the relative total scatter factor difference normalized to Monte Carlo and the x-axis represents the collimator diameter in millimeters. The continuous black line represents the Monte Carlo results and the dotted lines represent the uncertainties of the calculated $\Omega^{f_{\text{clin}},f_{\text{msr}}}_{Q_{\text{clin}},Q_{\text{msr}}}$ values.

for all the cones except the 5-mm cone, for which underresponses were evident. The best concordance with reference values was achieved with the 0.5-mm PSD. Another way to look at these data is to normalize them to Monte Carlo values as the reference dataset (as in Figs. 3 and 4). To achieve this, we introduce the relative difference between measured and calculated total scatter factors as expressed in Eq. (2). It is important to note that the local normalization may artificially exaggerate discrepancies:

$$y = \frac{s_{c,p\,\text{measured}} - s_{c,p\,\text{MC}}}{s_{c,p\,\text{MC}}} * 100. \qquad (2)$$

In Fig. 3, the dotted lines represent the Monte Carlo statistical uncertainties obtained by Araki.[8] All the measured values outside these dotted lines indicate that the discrepancies were not just statistical but real volume-averaging or perturbation effects. All the detectors, except the PTW 60008 silicon diode, rendered accurate results for cones with a diameter of 10 mm or higher (Fig. 3). The microLion and the 1.0-mm PSD showed a mean relative difference of 0.6% and 0.45% with Monte Carlo results, respectively, for all cones with a diameter larger than 5 mm. The 0.5-mm PSD measurements were inside the statistical uncertainties of the Monte Carlo simulations with all the cones with a mean relative difference of

TABLE I. Measured total scatter factors ($s_{c,p}$) using all the detectors studied in this work and calculated total scatter factors ($\Omega^{f_{\text{clin}},f_{\text{msr}}}_{Q_{\text{clin}},Q_{\text{msr}}}$) from Araki (Ref. 8) and Francescon *et al.* (Ref. 5). The relative uncertainties (%) are in parenthesis.

Cone size (mm)	PSD 0.5 (mm)	PSD 1.0 (mm)	PTW 60008	PTW 60012	MicroLion chamber	SFD diode	Araki (Ref. 8)	Francescon (Ref. 5)
5	0.679	0.675	0.717	0.708	0.668	0.712	0.685	0.682
	(0.39)	(0.24)	(0.06)	(0.03)	(0.00)	(0.28)	(1.00)	(1.4)
7.5	0.820	0.818	0.870	0.844	0.833	0.837	0.826	0.825
	(0.31)	(0.29)	(0.05)	(0.03)	(0.09)	(0.11)	(1.00)	(0.73)
10	0.873	0.870	0.911	0.887	0.885	0.879	0.881	0.880
	(0.31)	(0.23)	(0.08)	(0.08)	(0.06)	(0.07)	(1.00)	(0.68)
12.5	0.914	0.913	0.940	0.921	0.926	0.914	0.910	–
	(0.32)	(0.24)	(0.08)	(0.05)	(0.03)	(0.12)	(1.00)	
15	0.939	0.937	0.956	0.942	0.948	0.935	0.944	–
	(0.24)	(0.22)	(0.14)	(0.09)	(0.00)	(0.12)	(1.00)	
20	0.965	0.963	0.972	0.962	0.970	0.957	0.963	–
	(0.19)	(0.18)	(0.11)	(0.14)	(0.10)	(0.14)	(1.00)	
30	0.983	0.982	0.984	0.980	0.985	0.976	0.983	–
	(0.20)	(0.20)	(0.12)	(0.10)	(0.06)	(0.12)	(1.00)	
40	0.992	0.989	0.991	0.988	0.992	–	0.990	–
	(0.33)	(0.12)	(0.10)	(0.03)	(0.08)		(1.00)	
50	0.995	0.995	0.996	0.995	0.997	0.994	0.997	–
	(0.26)	(0.07)	(0.09)	(0.05)	(0.06)	(0.23)	(1.00)	
60	1	1	1	1	1	1	1	–
	(0.16)	(0.10)	(0.18)	(0.03)	(0.12)	(0.14)	(1.00)	

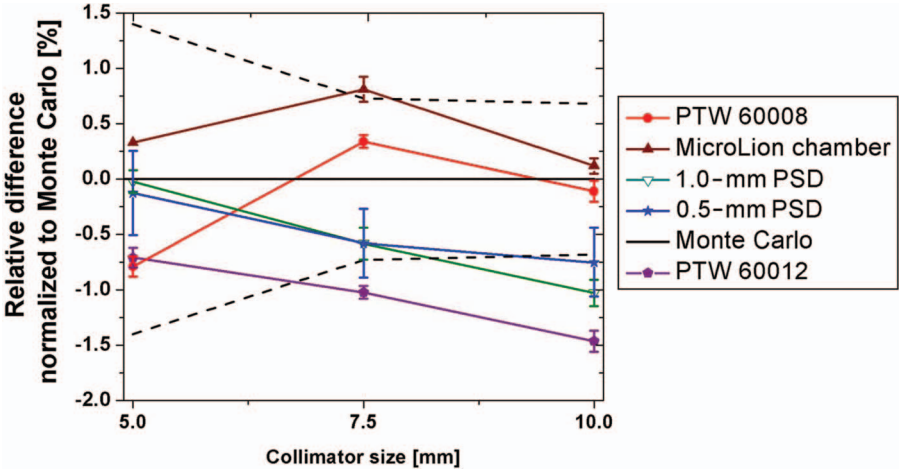

FIG. 5. Relative total scatter factors difference normalized to Monte Carlo [(Francescon *et al.* (Ref. 5)] for the corrected measurements. The y-axis represents the relative total scatter factor difference normalized to Monte Carlo and the x-axis represents the collimator diameter in millimeters. The continuous black line represents the Monte Carlo results and the dotted lines represent the uncertainties of the calculated $\Omega_{Q_{clin},Q_{msr}}^{f_{clin},f_{msr}}$ values.

0.44%. However, the electron spot size and the nominal electron energy incident on the target can vary from one accelerator to another, and thus influence total scatter factors for the smallest cones, as mentioned previously.[5] The electron spot size and the nominal electron energy incident on the target determined by Araki were not the same as those of the CyberKnife system used in the present study. Araki[8] fixed these parameters to 3.2 mm and 6.7 MeV, respectively, by fitting calculated and measured dose profiles and central axis depth-doses (Sec. II.D).

The procedure developed by Francescon *et al.*[5,36] allowed us to find an electron spot size of 2.2 ± 0.1 mm and an electron energy incident on the target of 6.6 ± 0.1 MeV for our specific CyberKnife system. Figure 4 presents the same results as those presented in Fig. 3 but compared to Francescon's values[5] with the determined parameters of our CyberKnife system. The simulation uncertainties (Monte Carlo) in Fig. 4 arose from three sources: the Monte Carlo statistical uncertainties (0.3%), the uncertainty of the electron spot size determination (±0.1 mm), and the uncertainty of the nominal electron energy determination (±0.1 MeV). The uncertainty using the 5-mm cone was the highest because the electron spot size determination uncertainty has the most substantial effect with this cone. The behavior of each detector relative to Monte Carlo simulations (i.e., over- or underresponse) is the same for Figs. 3 and 4, thus showing a consistency between both Monte Carlo studies used in this work. However, the magnitude of the difference between measured and actual total scatter factors in water should be more accurate using Francescon's calculations because our specific CyberKnife system parameters were determined.

Francescon *et al.*[5,36–38] modeled ten commercial detectors to determine correction factors ($k_{Q_{clin},Q_{msr}}^{f_{clin},f_{msr}}$, Eq. (1)) for the three smallest cones. Among these simulated detectors, the PTW 60008 diode, the PTW 60012 diode, and the microLion were used in the present study. These correction factors were applied to the measurements performed in this study, and the corrected values are presented in Fig. 5. Because no calculated correction factor existed for the PSDs, the volume-averaging effect was estimated for both PSDs by performing a two-dimensional integral, using the dose profiles measured during commissioning, as follows:

$$F_{\text{average}} = \frac{\int_0^{2\pi}\int_0^{d/2} D(r,\theta)\, r\, dr\, d\theta}{\pi d^2/4}. \quad (3)$$

Here, F_{average} is the average reading of the detector, d is the detector diameter perpendicular to the radiation beam, r and θ represent the position from the center in polar coordinates, and $D(r, \theta)$ is the relative dose value at the position r and θ normalized to the dose at the center of the field. The calculated volume-averaging correction factors are shown in Table II for all the detectors used. Applying the correction factors (volume-averaging only in the case of the PSDs, but Monte Carlo correction factors for the other detectors) importantly improved the agreement among all detector measurements and Monte Carlo values except those of the PTW 60012 diode. This latter detector was corrected using the factors calculated by Francescon *et al.* (2008).[5] Recently, Francescon *et al.* noticed that the epoxy density used to simulate the diodes to determine the correction factors was erroneous, so they performed an optimization to determine the correct density and correction factors were recalculated for the diodes considering this modification.[38] Using these new factors, a

TABLE II. Calculated volume-averaging correction factors [$1/F_{\text{average}}$ in Eq. (3)] for each detector.

Detector	5-mm cone diameter	7.5-mm cone diameter	10-mm cone diameter
0.5-mm PSD	1.003	1.001	1.000
1.0-mm PSD	1.011	1.002	1.001
PTW 60008	1.014	1.003	1.001
PTW 60012	1.014	1.003	1.001
MicroLion chamber	1.068	1.016	1.007
SFD diode	1.004	1.001	1.000

TABLE III. Correction factors $k_{Q_{clin},Q_{msr}}^{f_{clin},f_{msr}}$ for the PTW 60008 diode, the PTW 60012 diode, the SFD, and the microlion obtained using the 0.5-mm PSD as a reference dosimeter. The reference detector was corrected for the volume-averaging effect by using the calculated correction factors (Table II).

Detectors	Collimator diameter (mm)	Experimental correction factors	Literature	Difference (%)
PTW 60008 diode	5	0.950	0.944 (Ref. 36), 0.945 (Ref. 38)	−0.6, −0.5
	7.5	0.942	0.951 (Ref. 36), 0.960 (Ref. 38)	0.9, 1.8
	10	0.959	0.965 (Ref. 36), 0.974 (Ref. 38)	0.6, 1.5
PTW 60012 diode	5	0.963	0.957 (Ref. 5), 0.963 (Ref. 38)	−0.6, 0
	7.5	0.971	0.967 (Ref. 5), 0.975 (Ref. 38)	−0.4, 0.4
	10	0.985	0.978 (Ref. 5), 0.983 (Ref. 38)	−0.7, −0.2
SFD	5	0.957	0.952 (Ref. 8)	−0.5
	7.5	0.980	0.976 (Ref. 8)	−0.4
	10	0.994	–	–
MicroLion chamber	5	1.020	1.025 (Ref. 38)	0.5
	7.5	0.984	0.998 (Ref. 38)	1.4
	10	0.986	0.995 (Ref. 38)	0.9

better agreement was obtained between the PTW 60012 diode measurements and Monte Carlo values with relative differences of −0.09%, −0.20%, and −0.96% for the 5-, 7.5-, and 10-mm cones, respectively.

III.B. Correction factors $k_{Q_{clin},Q_{msr}}^{f_{clin},f_{msr}}$

Correction factors were also determined experimentally for the three smallest cones and for each detector using the 0.5-mm PSD as the reference dosimeter. Moreover, volume averaging was taken into account using Eq. (3) for the reference detector. The values obtained are shown in the third column of Table III. The fourth column represents correction factors found in the literature and obtained from different Monte Carlo studies of total scatter factors in small fields. Two calculated values are presented for the PTW diodes, and they represent the calculated correction factors reported by Francescon *et al.*[5,36,38] before and after the epoxy density optimization. The last column is the difference between the correction factors reported in the literature and those obtained in this study for each detector and for each collimator diameter. The experimental correction factors obtained in this work were within 2% of those obtained in different Monte Carlo studies.

III.C. Dose profiles

The measured dose profiles for the 5- and 60-mm cones, respectively, are shown in Figs. 6 and 7. Both PSDs dose profile measurements agreed over all the positions despite the fact that they provided different spatial resolutions. The silicon diode and the radiochromic film were in good agreement for the 5-mm cone dose profile, but the PSDs' responses were slightly higher for the first 2 mm from the center. These differences did not come from detectors' dose responses, but from water tank's mechanical arm positioning uncertainties. When the nominal uncertainty of ±0.1 mm provided by the manufacturer was applied to the PSDs' measurements, very good agreement was obtained between the PSDs and the other detectors. The silicon diode dose profiles showed in Figs. 6 and 7 did not suffer from this positioning error because several dose profiles were measured and averaged, minimizing this effect. For the 60-mm cone, very good agreement was obtained between all the detectors throughout the dose profile except in the tail, where the responses of the Gafchromic film and the diode were higher than those of the PSDs. Positioning errors were not noticeable using this cone because the dose profile was composed mainly of a nearly flat region (Fig. 7). Gamma evaluations were performed for both dose profiles measured using the 0.5-mm PSD as the reference detector (Figs. 6 and 7). The gamma evaluation was chosen to compare the detectors by measuring dose profiles because of possible PSDs positioning uncertainties mentioned previously. The 5-mm cone dose profile is mainly composed of penumbra, thus a positioning error of about 0.1 mm is

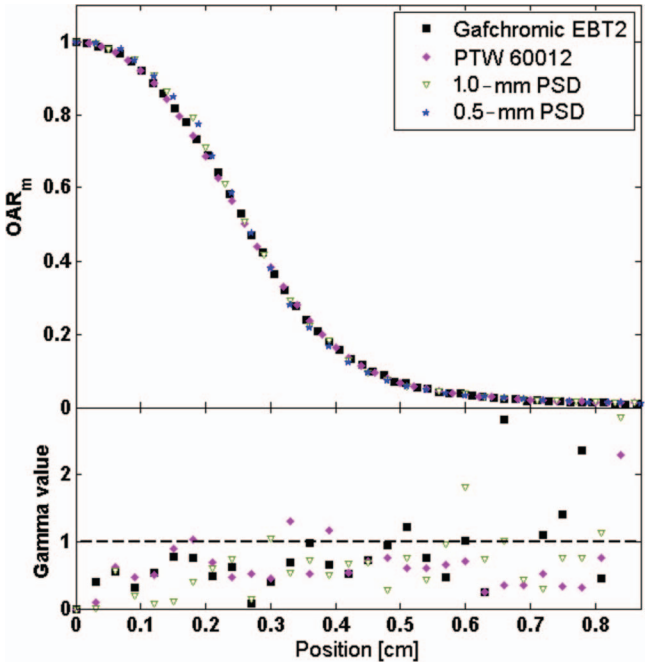

FIG. 6. Dose profile measured at 1.5 cm depth and 80 cm SAD with the 5-mm cone normalized to the dose measured at the center of the field. Error bars are not shown to simplify the visualization. The gamma evaluation used acceptance criteria of 2% and 0.2 mm.

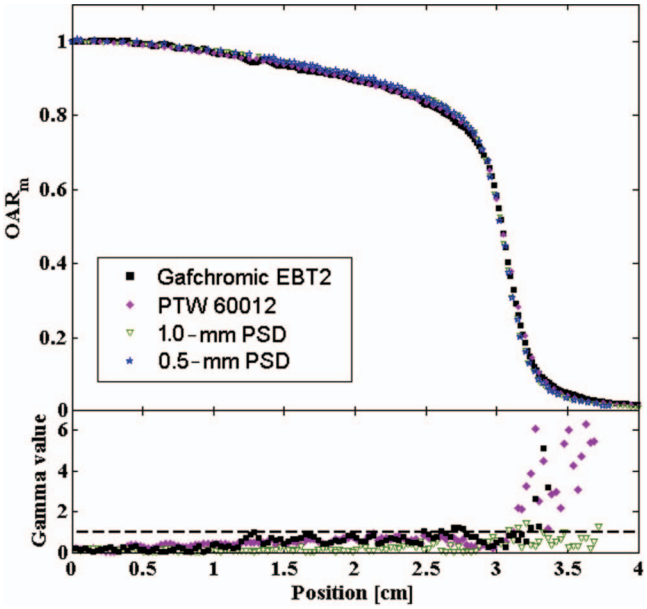

FIG. 7. Dose profile measured at 1.5 cm depth and 80 cm SAD with the 60-mm cone normalized to the dose measured at the center of the field. Error bars are not shown to simplify the visualization. The gamma evaluation used acceptance criteria of 2% and 0.2 mm.

similar to an error of about 5%–6% on the dose (Fig. 6). The acceptance criteria of these gamma evaluations were 2% on the local dose and 0.2 mm. The dose criterion was defined locally to verify whether the silicon diode over-responded in the tail of the dose profiles compared with the PSDs because of low photon energies. The spatial criterion was justified by the 0.1-mm uncertainty of the positioning arm (affecting the PSDs measurements).

IV. DISCUSSION

The measured total scatter factors using the PSDs showed very good agreement, within 1.5%, with those calculated in two different Monte Carlo studies. Correction factors were thus calculated for the commercial detectors used in this study using the 0.5-mm PSD as the detector of reference. These correction factors were within 2% of those calculated in different Monte Carlo studies showing the nonperturbing quality of PSD in the water-medium.

Table I shows that calculated total scatter factors obtained in both Monte Carlo studies are very similar. However, we expected a difference between Araki and Francescon of ~8% based on the work of Francescon *et al.*,[5] because of the difference on the electron spot size. There are probably differences in Monte Carlo simulations of the accelerator head because both studies defined the electron spot size in the same way, namely, the full width at half maximum of a radial Gaussian distribution.

Figure 3 suggests that the calculated $\Omega_{Q_{clin},Q_{msr}}^{f_{clin},f_{msr}}$ value was underestimated by about 1% by Araki for the 12.5-mm cone because all the detector measurements showed a discontinuity at this collimator size.

The behavior of the silicon diodes agreed with the results obtained by Dieterich and Sherouse[39] with the highest dose responses with the shielded diode and the lowest responses with the SFD in small fields (<20 mm). We implemented a strategy to minimize the signal drift with dose (SFD, Sec. II.B.1), thereby allowing us to compare the diodes on a similar basis. The measured total scatter factors using the SFD were lower than those using the other diodes for all the cones except the 5-mm, for which the PTW 60012 diode rendered the lowest value. Moreover, the measured total scatter factor using the PTW 60008 diode (shielded diode) was closer to the one obtained using the SFD for this cone. This effect is partially caused by the volume-averaging effect but mainly caused by the dose rate dependence of the PTW diodes.[40] The SFD is a dose rate-independent dosimeter, so its behavior in small fields is only the result of the silicon water nonequivalence and perturbation effects. Some studies have pointed out that the water nonequivalence of silicon leads to overestimation of the total scatter factors for the smallest radiosurgery fields.[8–10] The results obtained in the present study agree with those observations. Once the silicon diodes responses were corrected, good agreement was obtained between the measurements and the Monte Carlo calculations about total scatter factors for small fields (Fig. 5). On the other hand, all the silicon diodes agreed within 1% of the calculated total scatter factors for cones with a diameter of 20 mm or greater without any correction factor. Silicon diodes are widely used for radiosurgery system commissioning and QA measurements, thereby resulting in a slightly lower actual dose delivered to the patient for the smallest cones than that predicted by the planning system when no correction factor is applied to the measurements.

The microLion measurements were consistent with Araki's results for all cones except the 5-mm cone (Fig. 3). Considering that this dosimeter disagreed with only the smallest cone, analyzing this dosimeter using Francescon's results[5] was appropriate because of the determined electron spot size and electron nominal energy for our specific CyberKnife system. The volume-averaging effect was present for the microLion using the 5-mm cone having a dose response of about 2% under the calculated $\Omega_{Q_{clin},Q_{msr}}^{f_{clin},f_{msr}}$ (Fig. 4). However, it was determined by using Eq. (3) that an underestimation of 6% ($F_{average} = 0.937$) should be observed because of the volume-averaging effect with this detector and for this cone. This result implies that the dose response was partially compensated for by another effect causing an over-response, which was also slightly noticeable using the 7.5-mm cone. Francescon *et al.*[37,38] observed this small over-response in Monte Carlo simulations by finding a correction factor of 0.997 for a 7.5-mm field size despite the fact that the 2.5-mm diameter surface of the microLion sensitive volume still results in a non-negligible volume-averaging effect [estimated to 1.6% using Eq. (3)]. Ion recombination had a small effect (estimated to <1% using Fig. 2 of Pardo-Montero and Gómez[41]), but the over-responses came principally from perturbation effects of the detector because Monte Carlo simulations detected it (Monte Carlo does not simulate ion recombination). A recent Monte Carlo study suggested that the over-responses of the

microLion in small fields arose from the high-density material surrounding the sensitive volume.[42] MicroLion are good radiosurgery detectors but should be used carefully with the smallest fields because of the associated volume-averaging and perturbation effects.

PSDs measurements provided the best agreement with Monte Carlo simulations among all the detectors investigated. The volume-averaging effect probably caused the slight underestimation of the dose for the 5-mm cone using the 1.0-mm PSD because both PSDs' sensitive volumes were composed of polystyrene, and the 0.5-mm PSD dose response was within uncertainties of the calculated $\Omega_{Q_{\text{clin}},Q_{\text{msr}}}^{f_{\text{clin}},f_{\text{msr}}}$. Moreover, Fig. 5 shows that once the corrections were applied for the volume-averaging effect [Eq. (3)], the two PSDs agreed to within 0.1%. This means that the impact of a spatial resolution of 1.0-mm perpendicular to the radiation beam is about 1% on the 5-mm cone total scatter factor using a CyberKnife system. The excellent agreement obtained with Monte Carlo values suggests that PSDs are water equivalent and perturbation free detectors, the Čerenkov subtraction procedure used is accurate, and Francescon's procedure[5,36–38] for estimating the CyberKnife accelerator head parameters and correction factors is accurate. PSDs have proven that they are the only detectors that can render perturbation-free response relative to water in small radiation fields without correction factors and in real-time.

Correction factors using a PSD as the reference dosimeter were first proposed by Lacroix *et al.*[25,40] for depth-dose measurements. The concept was also adopted by Ralston *et al.*[43] to determine correction factors for silicon diodes by measuring total scatter factors for Varian Novalis beams. The measured total scatter factors in this study confirmed the excellent accuracy of the PSDs in small fields, making this concept interesting to apply to our measurements.

By comparing the dose profiles measured with the PTW 60012 diode to those measured with the PSDs, we can conclude that the impact of the water nonequivalence of the silicon diodes is negligible for small-field dose profile measurements (5-mm cone). The silicon diode showed a number of points passing the acceptance criteria (2%, 0.2 mm) similar to that for the 1.0-mm PSD using the 5-mm cone (Fig. 6). Moreover, Francescon *et al.*[37] determined, using Monte Carlo simulations, that the response of this diode model relative to water changes by less than 2% in the first 4.5 mm from the center using a 5-mm square field on a conventional linear accelerator. The results obtained in the present study agree with this observation. On the other hand, the silicon diode over-responded in the tail of the dose profile with the 60-mm cone having no point passing the acceptance criteria from about 3.1 to 3.8 mm from the center (Fig. 7). This over-response was probably caused by the high proportion of low-energy photons in this region.

The Gafchromic film had a very good acceptance passing rate (gamma evaluation) using the 5-mm cone as well. However, two points have been suppressed on the gamma evaluation (Fig. 6) having values of 13 and 15 (to 0.69 and 0.84 cm, respectively) to keep a good visualization of the other detectors. Excellent agreement was obtained between the Gafchromic film and the other detectors for the 60-mm cone dose profile (Fig. 7), but over-responses were noticeable in the tail as with the PTW 60012 diode. As explained in Sec. II.A.5, the Gafchromic film calibration curve was obtained using 13 dose points from 0 to 10 Gy. This calibration procedure did not characterize effectively the Gafchromic film response in low-dose region. Moreover, the films were used several months after the calibration curve determination. These two factors explain the discrepancies between the Gafchromic film and the PSDs measurements in the tail of the 60-mm cone dose profile.

Currently, the spatial resolution required to accurately measure small-field dose profiles is not well known, but the good agreement between the two PSDs indicates that a 1.0-mm diameter perpendicular to the radiation beam is sufficient down to a 5-mm field size. An excellent acceptance passing rate (gamma evaluation) was obtained using the 1.0-mm PSD for both profiles except in the tail of the 5-mm cone dose profile. Some points failed the gamma evaluation in this region, but the uncertainties of the 0.5-mm PSD were higher in this region.

V. CONCLUSIONS

We compared several stereotactic detectors by measuring total scatter factors and dose profiles. Currently available commercial detectors have limitations to perform accurate small-field dosimetry ($\leq$20 mm), and these limitations have been observed in the present study. We showed herein that silicon diodes are suitable for measuring dose profiles of the smallest field using a CyberKnife system (5-mm cone) despite the fact that they are water nonequivalent. However, their water nonequivalence causes over-responses in the tails of the larger fields available using a CyberKnife system. Moreover, important overestimations of the total scatter factors have been observed in small fields ($<$10 mm) with silicon diodes. The microLion under-responded to about 2.5% with the 5-mm cone because of a compensation for a volume-averaging effect and an over-response caused by the surrounding high-density material. Our findings show that small-field total scatter factors can be accurately measured using water-equivalent dosimeters like PSDs, which provided results similar to those of two independent Monte Carlo studies. Comparisons of two PSDs with different diameters perpendicular to the radiation beam suggested that using a 1.0-mm detector results in a negligible volume-averaging effect ($\approx$1%) down to a field size of 5 mm. PSDs are good candidates for reference radiosurgery detectors for measurements requiring water equivalence, such as total scatter factors, tissue-phantom ratios, percent depth-doses, and total treatment delivery verification.

ACKNOWLEDGMENTS

This research is supported in part by the Natural Science and Engineering Research Council of Canada (NSERC) support Grant No. 262105. Jonathan Morin is financially supported by a NSERC and a FQRNT postgraduate scholarship.

The authors are grateful to Frédéric Lacroix for providing expertise with radiochromic films.

[a]Author to whom correspondence should be addressed. Electronic mail: beaulieu@phy.ulaval.ca

[1]E. B. Podgorsak, *Radiation Oncology Physics: A Handbook for Teachers and Students*, 1st ed. (International Atomic Energy Agency, Vienna, 2005).
[2]S. D. Chang, W. Main, D. P. Martin, I. C. Gibbs, and M. P. Heibrun, "An analysis of the accuracy of the CyberKnife: A robotic frameless stereotactic radiosurgical system," Neurosurgery **52**, 140–147 (2003).
[3]C. Antypas and E. Pantelis, "Performance evaluation of a Cyberknife® G4 image-guided robotic stereotactic radiosurgery system," Phys. Med. Biol. **53**, 4697–4718 (2008).
[4]D. M. Duggan and C. W. Coffey II, "Small photon field dosimetry for stereotactic radiosurgery," Med. Dosim. **23**, 153–159 (1998).
[5]P. Francescon, S. Cora, and C. Cavedon, "Total scatter factors of small beams: A multidetector and Monte Carlo study," Med. Phys. **35**, 504–513 (2008).
[6]R. Alfonso, P. Andreo, R. Capote, M. S. Huq, W. Kilby, P. Kjäll, T. R. Mackie, H. Palmans, K. Rosser, J. Seuntjens, W. Ullrich, and S. Vatnitsky, "A new formalism for reference dosimetry of small and nonstandard fields," Med. Phys. **35**, 5179–5186 (2008).
[7]W. U. Laub and T. Wong, "The volume effect of detectors in the dosimetry of small fields used in IMRT," Med. Phys. **30**, 341–347 (2003).
[8]F. Araki, "Monte Carlo study of a Cyberknife stereotactic radiosurgery system," Med. Phys. **33**, 2955–2963 (2006).
[9]M. Heydarian, P. W. Hoban, and A. H. Beddoe, "A comparison of dosimetry techniques in stereotactic radiosurgery," Phys. Med. Biol. **41**, 93–110 (1996).
[10]F. Haryanto, M. Fippel, W. Laub, O. Dohm, and F. Nüsslin, "Investigation of photon beam output factors for conformal radiation therapy—Monte Carlo simulations and measurements," Phys. Med. Biol. **47**, N133–N143 (2002).
[11]S. Dieterich, C. Cavedon, C. F. Chuang, A. B. Cohen, J. A. Garrett, C. L. Lee, J. R. Lowenstein, M. F. d'Souza, D. D. Taylor, Jr., X. Wu, and C. Yu, "Report of AAPM TG 135: Quality assurance for robotic radiosurgery," Med. Phys. **38**, 2914–2936 (2011).
[12]O. A. Sauer and J. Wilbert, "Measurement of output factors for small photon beams," Med. Phys. **34**, 1983–1988 (2007).
[13]K. Jordan, "Review of recent advances in non gel dosimeters," J. Phys.: Conf. Ser. **56**, 132–141 (2006).
[14]A. S. Beddar, T. J. Kinsella, A. Ikhlef, and C. H. Sibata, "A miniature "Scintillator-Fiberoptic-PMT" detector system for the dosimetry of small fields in stereotactic radiosurgery," IEEE Trans. Nucl. Sci. **48**, 924–928 (2001).
[15]M. Guillot, L. Beaulieu, L. Archambault, S. Beddar, and L. Gingras, "A new water-equivalent 2D plastic scintillation detectors array for the dosimetry of megavoltage energy photon beams in radiation therapy," Med. Phys. **38**, 6763–6774 (2011).
[16]J.-C. Gagnon, D. Theriault, M. Guillot, L. Archambault, S. Beddar, L. Gingras, and L. Beaulieu, "Dosimetric performance and array assessment of plastic scintillation detectors for stereotactic radiosurgery quality assurance," Med. Phys. **39**, 429–436 (2012).
[17]D. Letourneau, J. Pouliot, and R. Roy, "Miniature scintillating detector for small field radiation therapy," Med. Phys. **26**, 2555–2561 (1999).
[18]D. M. Klein, R. C. Tailor, L. Archambault, L. Wang, F. Therriault-Proulx, and A. S. Beddar, "Measuring output factors of small fields formed by collimator jaws and multileaf collimator using plastic scintillation detectors," Med. Phys. **37**, 5541–5549 (2010).
[19]A. R. Beierholm, R. O. Ottosson, L. R. Lindvold, C. F. Behrens, and C. E. Andersen, "Characterizing a pulse-resolved dosimetry system for complex radiotherapy beams using organic scintillators," Phys. Med. Biol. **56**, 3033–3045 (2011).
[20]S. Derreumaux, C. Bassinet, C. Huet, M. Chea, G. Boisserie, G. Brunet, M. Baumann, F. Trompier, P. Roch, and I. Clairand, "Su-e-t-163: Characterization of the response of active detectors and passive dosemeters used for dose measurement in small photon beams," Med. Phys. **38**, 3523–3523 (2011).
[21]I. Griessbach, M. Lapp, J. Bohsung, G. Gademann, and D. Harder, "Dosimetric characteristics of a new unshielded silicon diode and its application in clinical photon and electron beams," Med. Phys. **32**, 3750–3754 (2005).
[22]B. Arjomandy, R. Tailor, A. Anand, N. Sahoo, M. Gillin, K. Prado, and M. Vicic, "Energy dependence and dose response of Gafchromic EBT2 film over a wide range of photon, electron, and proton beam energies," Med. Phys. **37**, 1942–1947 (2010).
[23]H. Bouchard and F. Lacroix, "SU-GG-T-329: Gafgui: An open-source project for radiochromic film dosimetry," Med. Phys. **37**, 3261–3262 (2010).
[24]H. Bouchard, F. Lacroix, G. Beaudoin, J.-F. Carrier, and I. Kawrakow, "On the characterization and uncertainty analysis of radiochromic film dosimetry," Med. Phys. **36**, 1931–1946 (2009).
[25]F. Lacroix, M. Guillot, M. McEwen, C. Cojocaru, L. Gingras, A. S. Beddar, and L. Beaulieu, "Extraction of depth-dependent perturbation factors for parallel-plate chambers in electron beams using a plastic scintillation detector," Med. Phys. **37**, 4331–4342 (2010).
[26]E. Chung, S. Davis, and J. Seuntjens, "Ion recombination in a liquid-filled ionization chamber in high-energy photon beams," presented at the *54th Annual Meeting of the AAPM*, Charlotte, NC, July 29 – August 2, 2012).
[27]A. S. Beddar, D. J. Mason, and P. F. O'Brien, "Absorbed dose perturbation caused by diodes for small field photon dosimetry," Med. Phys. **21**, 1075–1079 (1994).
[28]A. S. Beddar, T. R. Mackie, and F. H. Attix, "Cerenkov light generated in optical fibres and other light pipes irradiated by electron beams," Phys. Med. Biol. **37**, 925–935 (1992).
[29]S. F. de Boer, A. S. Beddar, and J. A. Rawlinson, "Optical filtering and spectral measurements of radiation-induced light in plastic scintillation dosimetry," Phys. Med. Biol. **38**, 945–958 (1993).
[30]A. S. Beddar, T. R. Mackie, and F. H. Attix, "Water-equivalent plastic scintillation detectors for high-energy beam dosimetry. I. Physical characteristics and theoretical considerations," Phys. Med. Biol. **37**, 1883–1900 (1992).
[31]J. M. Fontbonne, G. Iltis, G. Ban, A. Battala, J. C. Vernhes, J. Tillier, N. Bellaize, C. Le Brun, B. Tamain, K. Mercier, and J. C. Motin, "Scintillating fiber dosimeter for radiation therapy accelerator," IEEE Trans. Nucl. Sci. **49**, 2223–2227 (2002).
[32]A.-M. Frelin, J. M. Fontbonne, G. Ban, J. Colin, and M. Labalme, "Spectral discrimination of Čerenkov radiation in scintillating dosimeters," Med. Phys. **32**, 3000–3006 (2005).
[33]M. Guillot, L. Gingras, L. Archambault, S. Beddar, and L. Beaulieu, "Spectral method for the correction of the Cerenkov light effect in plastic scintillation detectors: A comparison study of calibration procedures and validation in Cerenkov light-dominated situations," Med. Phys. **38**, 2140–2150 (2011).
[34]K. J. Jordan, "Evaluation of ruby as a fluorescent sensor for optical fiber-based radiation dosimetry," Proc. SPIE **2705**, 170–178 (1996).
[35]M. A. Clift, P. N. Johnston, and D. V. Webb, "A temporal method of avoiding the Cerenkov radiation generated in organic scintillator dosimeters by pulsed mega-voltage electron and photon beams," Phys. Med. Biol. **47**, 1421–1433 (2002).
[36]P. Francescon, S. Cora, C. Cavedon, and P. Scalchi, "Application of a Monte Carlo-based method for total scatter factors of small beams to new solid state micro-detectors," J. Appl. Clin. Med. Phys. **10**, 147–152 (2009).
[37]P. Francescon, S. Cora, and N. Satariano, "Calculation of $k_{Q_{clin},Q_{msr}}^{f_{clin},f_{msr}}$ for several small detectors and for two linear accelerators using Monte Carlo simulations," Med. Phys. **38**, 6513–6527 (2011).
[38]P. Francescon, W. Kilby, N. Satariano, and S. Cora, "Monte Carlo simulated correction factors for machine specific reference field dose calibration and output factor measurement using fixed and iris collimators on the CyberKnife system," Phys. Med. Biol. **57**, 3741–3758 (2012).
[39]S. Dieterich and G. W. Sherouse, "Experimental comparison of seven commercial dosimetry diodes for measurement of stereotactic radiosurgery cone factors," Med. Phys. **38**, 4166–4173 (2011).
[40]F. Lacroix, M. Guillot, M. McEwen, L. Gingras, and L. Beaulieu, "Extraction of depth-dependent perturbation factors for silicon diodes using a plastic scintillation detector," Med. Phys. **38**, 5441–5447 (2011).
[41]J. Pardo-Montero and F. Gomez, "Determining charge collection efficiency in parallel-plate liquid ionization chambers," Phys. Med. Biol. **54**, 3677–3689 (2009).
[42]T. Underwood, H. Winter, J. Fenwick, and M. Hill, "Modifying detector designs for small field dosimetry," paper presented at the ESTRO 31, Barcelona, Spain, 9–13 May 2012.
[43]A. Ralston, P. Liu, K. Warrener, D. McKenzie, and N. Suchowerska, "Small field diode correction factors derived using an air core fibre optic scintillation dosimeter and EBT2 film," Phys. Med. Biol. **57**, 2587–2602 (2012).